

Diffusion-Pretrained Dense and Contextual Embeddings

Sedigheh Eslami^{*,1}, Maksim Gaiduk^{*,1}, Markus Krimmel^{*,1}, Louis Milliken^{*,1}, Bo Wang^{*,1} and Denis Bykov¹

^{*}Equal contributions, ¹Perplexity AI

Abstract

In this report, we introduce pplx-embed, a family of multilingual embedding models that employ multi-stage contrastive learning on a diffusion-pretrained language model backbone for web-scale retrieval. By leveraging bidirectional attention through diffusion-based pretraining, our models capture comprehensive bidirectional context within passages, enabling the use of mean pooling and a late chunking strategy to better preserve global context across long documents. We release two model types: pplx-embed-v1 for standard retrieval, and pplx-embed-context-v1 for contextualized embeddings that incorporate global document context into passage representations. pplx-embed-v1 achieves competitive performance on the MTEB(Multilingual, v2), MTEB(Code), MIRACL, BERGEN, and ToolRet retrieval benchmarks, while pplx-embed-context-v1 sets new records on the ConTEB benchmark. Beyond public benchmarks, pplx-embed-v1 demonstrates strong performance on our internal evaluation suite, which focuses on real-world, large-scale search scenarios over tens of millions of documents. These results validate the models' effectiveness in production environments where retrieval quality and efficiency are critical at scale.

1. Introduction

Dense textual embeddings represent texts as points in a continuous vector space in which distances capture meaningful semantic relationships. Embeddings are a crucial part of search systems, as they map queries and documents into a shared semantic space, in which information can be retrieved efficiently via approximate nearest neighbor search. The recent development of large language models has increasingly shifted embedding model training toward employing pretrained decoder-only LLMs to leverage their pre-existing knowledge and improve embedding quality (Jiang et al., 2024; Lee et al., 2025b; Zhang et al., 2025b). We investigate diffusion-based language models (Austin et al., 2021; Nie et al., 2025b) as an alternative paradigm. Diffusion language models employ transformer encoders with bidirectional attention, enabling more comprehensive context modeling compared to causally masked autoregressive models (Zhang et al., 2025a). This architectural difference is particularly advantageous for retrieval tasks, where capturing the global document context is essential.

This report introduces pplx-embed¹, a family of multilingual text embedding models employing multi-stage contrastive learning on a diffusion-pretrained language model backbone for web-scale retrieval. Continued pretraining via a diffusion objective converts a

¹<https://huggingface.co/collections/perplexity-ai/pplx-embed>

causally masked LLM backbone into a bidirectional encoder. Further contrastive training on large-scale question-document pairs, as well as triplet data, aligns the embedding space geometry with semantic similarity. We release two model types: pplx-embed-v1 for standard retrieval and pplx-embed-context-v1 for encoding passages with respect to document-level context. Both models are released in 0.6B- and 4B-parameter scales. Notably, our models are not instruction-tuned, eliminating the need for users to maintain instruction prefixes.

The pplx-embed family utilizes native quantization-aware training and outputs INT8 embeddings by default, achieving competitive performance while offering significantly improved efficiency. On MTEB(Multilingual, v2) (Enevoldsen et al., 2025; Muennighoff et al., 2023), pplx-embed-v1-4B achieves an average nDCG@10 of 69.66% with INT8 quantization, matching or exceeding leading models such as Qwen3-Embedding-4B (69.60%) and gemini-embedding-001 (67.71%). The pplx-embed-v1-4B model also demonstrates competitive performance on the MTEB(Code) and MIRACL benchmarks (Zhang et al., 2023). For contextual retrieval on ConTEB (Conti et al., 2025), pplx-embed-context-v1-4B outperforms state-of-the-art contextual models such as voyage-context-3² (79.45%) and Anthropic Contextual³ (72.4%) with an average nDCG@10 of 81.96%. On ToolRet (Shi et al., 2025), pplx-embed-v1-4B achieves 44.45% average nDCG@10, surpassing larger 7B models including NV-Embed-v1 (Lee et al., 2025a) (42.71%) and GritLM-7B (Muennighoff et al., 2025) (41.13%). This enables efficient pre-filtering of relevant tools from large API corpora, reducing context usage. We demonstrate that pplx-embed-v1 consistently outperforms BGE-M3 (Chen et al., 2024) and Qwen3-Embedding on the large-scale BERGEN (Rau et al., 2024) RAG benchmark, with pplx-embed-v1-0.6B beating the larger Qwen3-Embedding-4B model on three of the five question-answering tasks. We further describe internal benchmarks for assessing embedding models as first-stage retrievers at web-scale and show superior performance of pplx-embed-v1 in comparison to Qwen3-Embedding and BGE-M3.

2. PPLX Embedding

This section presents our training framework for learning high-quality embeddings for retrieval through a multi-stage curriculum. We combine four distinct training paradigms in a branched fashion, followed by a merging and selection stage. A schematic illustration of our training process is provided in Figure 1.

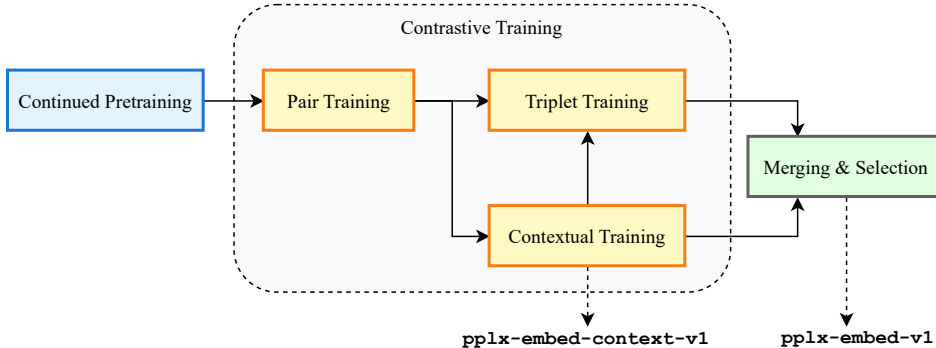


Figure 1 | Training pipeline of pplx-embed-v1 and pplx-embed-context-v1.

²<https://blog.voyageai.com/2025/07/23/voyage-context-3/>

³<https://www.anthropic.com/engineering/contextual-retrieval>

In the first training stage, described in Section 2.1, we perform continued pretraining of a decoder-only transformer on a diffusion objective, allowing it to use bidirectional self-attention. Subsequent training on query-document pairs (Section 2.3) establishes basic semantic alignment of sequence-level embeddings. Following this, a contextual stage (Section 2.4) trains chunk-level embeddings, allowing the model to identify relevant passages within documents. The pplx-embed-context-v1 model is obtained from this training stage. We perform triplet training with hard negatives (Section 2.5) on checkpoints obtained after pair and contextual training, refining boundaries between similar but non-relevant documents. For model merging, we employ Spherical Linear Interpolation (Shoemaker, 1985) of the contextual model and the triplet checkpoints to obtain pplx-embed-v1.

2.1. Continued Diffusion Pretraining

Following the methodology of Gong et al. (2025), we train two bidirectional diffusion language models via continued pretraining of existing autoregressive decoder-only backbones. Considering the state-of-the-art performance of the Qwen3 family (Yang et al., 2025), we choose Qwen3-0.6B⁴ and 4B⁵ as our base models.

We disable causal attention masking and train the resulting transformer encoders to reverse a corrupting noise process. We adopt a continuous-time formulation (Shi et al., 2024) and an absorbing state process in which, at timestep $t \in [0, 1]$, each token has decayed to the absorbing [MASK] state independently with probability t . To represent the [MASK] state, we repurpose a rarely used token from the Qwen3 vocabulary. Following prior work (Gong et al., 2025; Nie et al., 2025b; Ye et al., 2025), we preserve the left-shift operation that is applied during autoregressive pretraining. Although we also performed experiments with annealing the causal attention mask (Gong et al., 2025), we did not observe substantial performance improvements and did not pursue this technique further.

During training, we sample $t \sim \mathcal{U}(0.001, 1)$ for each input sequence independently and mask each token in the input sequence with probability t . We train our models via the standard evidence lower bound, which is given by the sum of token-wise cross entropies at masked positions, scaled by $1/t$.

Half of our training data consists of English educational web pages from FineWeb-Edu (Penedo et al., 2024), while the other half covers 29 other languages with data sourced from FineWeb2 (Penedo et al., 2025) and FineWeb2-HQ (Messmer et al., 2025). We train our models for 60,000 steps with a global batch size of 1024 and a sequence length of 4096. Thus, we perform pretraining on approximately 250 billion tokens of multilingual text data. Following Nie et al. (2025a), we truncate 1% of the training sequences to a randomly chosen length to ensure that the models are exposed to varying sequence lengths. We use an AdamW optimizer (Loshchilov and Hutter, 2019) with a warmup-stable-decay schedule and peak learning rates of 5×10^{-4} and 3.16×10^{-4} for the 0.6B and 4B models, respectively. For a more detailed description of hyperparameters, we refer the reader to Appendix A. We leverage the resulting models exclusively for contrastive learning, evaluating them solely on embedding quality rather than generative performance.

⁴<https://huggingface.co/Qwen/Qwen3-0.6B-Base>

⁵<https://huggingface.co/Qwen/Qwen3-4B-Base>

2.2. Pooling and Quantization

To produce embeddings, we pool token-level representations extracted from the backbone model into a sequence-level representation. While recent embedding models based on decoder-only transformers (Tang and Yang, 2024; Zhang et al., 2025b) typically employ last-token pooling, our bidirectional architecture allows the application of mean pooling. We propose a pooling method that natively combines mean pooling with quantization. Given token-wise embeddings $(\mathbf{v}_l)_{l=1}^L \in \mathbb{R}^{L \times d}$ for a sequence of length L , we define the sequence-level embedding as:

$$\left\lfloor 127 \cdot \tanh \left(\frac{1}{L} \sum_{l=1}^L \mathbf{v}_l \right) + \frac{1}{2} \right\rfloor.$$

The resulting vector has integer entries in $\{-127, \dots, 127\}$, which are representable as signed 8-bit integers. We employ the quantization above not only during inference, but also during all contrastive training stages. We use straight-through gradient estimation (Bengio et al., 2013) to backpropagate through the non-differentiable rounding operation. The quantized embeddings are compared via their cosine similarity.

We also support binary quantization, which reduces the size of output embeddings by setting each entry of the mean-pooled embedding vector to -1 or 1 :

$$\text{bin}(x) = \begin{cases} 1 & \text{if } x \geq 0, \\ -1 & \text{otherwise.} \end{cases}$$

While an embedding model could be trained using binary quantization with straight-through gradient estimation, we find that training-free post-hoc binarization can be applied with minimal performance loss.

2.3. Pair Training

Pair training represents the first contrastive learning stage, establishing foundational semantic alignment between queries and documents. The model learns to maximize the similarity of queries with their corresponding documents and minimize the similarity with unrelated ones. We employ an InfoNCE contrastive loss, which contrasts queries simultaneously against in-batch documents and other in-batch queries. Given a set of N query-document pairs, we obtain corresponding embedding vectors $\mathbf{q}_i \in \mathbb{R}^d$ and $\mathbf{d}_i \in \mathbb{R}^d$ from our encoder for $i = 1, \dots, N$. For a temperature $\tau > 0$, the loss is defined as:

$$\mathcal{L}^{\text{pair}} = -\frac{1}{N} \sum_{i=1}^N \log \frac{e^{s(\mathbf{q}_i, \mathbf{d}_i)/\tau}}{e^{s(\mathbf{q}_i, \mathbf{d}_i)/\tau} + \sum_{j \neq i}^N m_i(\mathbf{d}_j) e^{s(\mathbf{q}_i, \mathbf{d}_j)/\tau} + \sum_{j \neq i}^N m_i(\mathbf{q}_j) e^{s(\mathbf{q}_i, \mathbf{q}_j)/\tau}},$$

with $m_i(\mathbf{x}) = \mathbb{1}_{\{s(\mathbf{q}_i, \mathbf{x}) \leq s(\mathbf{q}_i, \mathbf{d}_i) + 0.1\}}$ masking some terms, and $s(\mathbf{q}_i, \mathbf{d}_i) = \frac{\mathbf{q}_i \cdot \mathbf{d}_i}{\|\mathbf{q}_i\|_2 \|\mathbf{d}_i\|_2}$ being the cosine similarity. Inspired by Zhang et al. (2025b), we design the masking function m to mitigate the effects of false negative samples. It compares the similarity of each in-batch negative to the query against that of the positive pair. When a negative sample's similarity exceeds that of the positive pair by more than 0.1, indicating potential semantic relevance, and thus a likely false negative, the function masks its contribution, thereby preventing distortion of the learned representation space.

Pair training is conducted in three steps to gradually incorporate non-English data: first, the model is trained only on English, then on English and cross-lingual data, and finally on the entire pair dataset containing multilingual samples. More details on the training setup are provided in Appendix B.

2.4. Contextual Training

Contextual training is an approach for training embedding models on long documents divided into chunks such that the embedding of each chunk retains contextual information from the whole document. Given N query-document pairs where each document contains C chunks, $d_i = \{c_{ik}\}_{k=1}^C$, we compute embedding vectors $\mathbf{c}_{ik} \in \mathbb{R}^d$ for chunk k from document i . We use a dual-objective loss function to capture local chunk-level semantics as well as global document-level representations. Inspired by [Conti et al. \(2025\)](#), we define the local loss as a combination of the in-batch and in-sequence losses for chunks. For the in-sequence contrastive loss, the target (gold) chunk from a document is treated as the positive sample, and all remaining chunks from the same document are used as negatives. In contrast, for the in-batch loss, the gold chunk remains the positive sample, but the negatives are defined as all other chunks in the batch, including those from the same document. Using mean pooling and INT8 quantization to obtain the chunk-level embeddings, we define the sequence loss as:

$$\mathcal{L}^{\text{seq}} = -\frac{1}{N} \sum_{i=1}^N \log \frac{e^{s(\mathbf{q}_i, \mathbf{c}_{i*})/\tau}}{\sum_{k=1}^C e^{s(\mathbf{q}_i, \mathbf{c}_{ik})/\tau}},$$

with \mathbf{c}_{i*} representing the embedding of the gold chunk. Furthermore, the in-batch loss is:

$$\mathcal{L}^{\text{batch}} = -\frac{1}{N} \sum_{i=1}^N \log \frac{e^{s(\mathbf{q}_i, \mathbf{c}_{i*})/\tau}}{\sum_{j=1}^N \sum_{k=1}^C e^{s(\mathbf{q}_i, \mathbf{c}_{jk})/\tau}}.$$

The final local loss is then calculated by:

$$\mathcal{L}^{\text{local}} = \alpha \mathcal{L}^{\text{seq}} + (1 - \alpha) \mathcal{L}^{\text{batch}}.$$

In our experiments, we set $\alpha = 0.2$.

For the global loss, we employ an InfoNCE objective to model query-document similarities. However, multiple queries within a batch may correspond to the same document, which would erroneously treat duplicate documents as negatives and introduce false negatives during training. To mitigate this, we identify and mask duplicate documents in the batch by comparing their hashes. Let $h(d)$ be a hash function mapping documents to identifiers (e.g., MD5). We introduce a duplicate indicator masking matrix M^{dup} :

$$M_{ij}^{\text{dup}} = \begin{cases} 0, & \text{if } h(d_i) = h(d_j) \text{ and } i \neq j, \\ 1, & \text{otherwise.} \end{cases}$$

Similar to the pair loss, we apply similarity threshold masking and include query-query negatives. Combining these with duplicate document masking, we define the global loss as:

$$\mathcal{L}^{\text{global}} = -\frac{1}{N} \sum_{i=1}^N \log \frac{e^{s(\mathbf{q}_i, \mathbf{d}_i)/\tau}}{\sum_{j=1}^N M_{ij}^{\text{dup}} m_i(\mathbf{d}_j) e^{s(\mathbf{q}_i, \mathbf{d}_j)/\tau} + \sum_{j \neq i}^N m_i(\mathbf{q}_j) e^{s(\mathbf{q}_i, \mathbf{q}_j)/\tau}}.$$

For the total loss, pplx-embed-context-v1 combines local and global losses with a scheduled weight β . We use a cosine schedule starting at $\beta = 0.2$ with a final target value of 0.5. The goal is for the model to first focus on learning local chunk-level semantics and gradually include document-level learning to mitigate forgetting of coarse document-level semantics. The total loss is defined as:

$$\mathcal{L}^{\text{context}} = \beta \mathcal{L}^{\text{global}} + (1 - \beta) \mathcal{L}^{\text{local}}.$$

We provide details of the training setup in Appendix B.

2.5. Triplet Training

Triplet training extends traditional pairwise contrastive learning by incorporating explicit hard negative examples alongside positive documents, enabling models to learn more discriminative embeddings through fine-grained relevance distinctions. Given a set of N query-document triplets, we compute embeddings $\{\mathbf{d}_{ik}^h \in \mathbb{R}^d\}_{k=1}^K$ corresponding to the hard negatives of the query $\mathbf{q}_i \in \mathbb{R}^d$. The triplet contrastive InfoNCE loss is then formulated as:

$$\mathcal{L}^{\text{triplet}} = -\frac{1}{N} \sum_{i=1}^N \log \frac{e^{s(\mathbf{q}_i, \mathbf{d}_i)/\tau}}{\sum_{j=1}^N e^{s(\mathbf{q}_i, \mathbf{d}_j)/\tau} + \sum_{j=1}^N \sum_{k=1}^K e^{s(\mathbf{q}_i, \mathbf{d}_{jk}^h)/\tau}}.$$

For more details on the training setup, we refer the reader to Appendix B.

2.6. Datasets for Contrastive Learning

For contrastive training, we employ English, multilingual, and synthetic datasets. The final set contains 65.6% English, 6.7% cross-lingual, 1% code, and 26.7% multilingual samples from 60 different languages. Contextual training is performed on the ConTEB training data, as well as data synthesized from the MLDR training set. Triplet training uses considerably less but higher-quality data, spanning 12 datasets. Of this data, 92% is English, 1% is code, and 7% consists of multilingual text covering 15 different languages.

All synthetic training data are generated using LLM-based synthesis with the Qwen3-30B-A3B-Instruct-2507 model. Inspired by [Zhang et al. \(2025b\)](#), our synthesis pipeline employs a two-stage persona-based approach to create diverse query-document pairs from web-scale corpora based on the top-5 relevant personas. For contextual training, we utilize a similar pipeline that generates synthetic queries for passages in a given document.

3. Evaluations

We evaluate our models across diverse benchmarks spanning multiple domains and languages. Our evaluation suite focuses on retrieval tasks using public and in-house datasets. In Section 3.1, we report results on the well-established MTEB ([Enevoldsen et al., 2025](#); [Muennighoff et al., 2023](#)), MIRACL ([Zhang et al., 2023](#)), ConTEB ([Conti et al., 2025](#)), BERGEN ([Rau et al., 2024](#)), and ToolRet ([Shi et al., 2025](#)) benchmarks, providing a holistic measure of embedding quality across domains. In Section 3.2, we describe internal benchmarks designed as realistic indicators of the performance of embedding models in web-scale retrieval systems.

Table 1 | Storage efficiency (document embeddings per megabyte, higher is better) and average performance (nDCG@10) on multilingual and code retrieval tasks. Upper group: models >1B or unknown parameters; lower group: models <1B parameters. The best score per group is in bold, second-best score underlined.

| Model | Docs/MB | MTEB(Multilingual, v2) | MTEB(Code) |
|------------------------------------|--------------|------------------------|--------------|
| pplx-embed-v1-4B (INT8) | <u>390</u> | 69.66 | <u>78.73</u> |
| pplx-embed-v1-4B (BIN) | 3,125 | 68.22 | 78.11 |
| qwen3-embed-4B | 97 | <u>69.60</u> | 80.07 |
| gemini-embedding-001 | 81 | 67.71 | 76.00 |
| text-embedding-3-large | 81 | 59.27 | 66.54 |
| pplx-embed-v1-0.6B (INT8) | <u>976</u> | 65.41 | 75.85 |
| pplx-embed-v1-0.6B (BIN) | 7,812 | 61.44 | 73.91 |
| qwen3-embed-0.6B | 244 | <u>64.65</u> | 75.42 |
| embed-gemma-0.3B | 325 | 62.58 | 68.76 |

Table 2 | nDCG@10 on the MIRACL RetrievalHardNegatives task per language.

| Model | Docs/MB | Avg | ar | bn | de | en | es | fa | fi | fr | hi | id | ja | ko | ru | sw | te | th | yo | zh |
|------------------------------------|--------------|-------------|-------------|-------------|-------------|-------------|-------------|-------------|-------------|-------------|-------------|-------------|-------------|-------------|-------------|-------------|-------------|-------------|-------------|-------------|
| pplx-embed-v1-4B (INT8) | <u>390</u> | 66.2 | 74.5 | 74.7 | 58.9 | 55.8 | 55.2 | 57.7 | 76.8 | 55.8 | 60.5 | 51.1 | 68.7 | 68.2 | 68.2 | <u>71.4</u> | 78.8 | 74.6 | 80.2 | 61.3 |
| pplx-embed-v1-4B (BIN) | 3,125 | 64.6 | 73.3 | 73.1 | 55.8 | 54.9 | 53.1 | 56.7 | 74.9 | 55.1 | 58.6 | 49.7 | 66.2 | 66.3 | 65.8 | 70.6 | 77.2 | 73.3 | 79.4 | 59.6 |
| gemini-embedding-001 | 81 | 70.4 | 78.8 | 79.3 | <u>60.7</u> | <u>59.0</u> | <u>57.5</u> | <u>61.6</u> | <u>77.5</u> | <u>56.3</u> | <u>65.1</u> | <u>54.4</u> | 75.5 | 69.2 | 74.0 | 81.3 | <u>80.7</u> | 81.3 | 89.1 | 66.4 |
| qwen3-embed-4B | 97 | 69.5 | <u>78.6</u> | <u>78.3</u> | 63.0 | 59.6 | 58.9 | 62.2 | 77.5 | 60.2 | <u>64.2</u> | 56.8 | <u>72.5</u> | <u>69.1</u> | <u>71.7</u> | 68.9 | 84.1 | <u>79.9</u> | <u>80.3</u> | <u>65.1</u> |
| text-embedding-3-large | 81 | 56.9 | 69.1 | 52.4 | 52.6 | 53.5 | 51.9 | 41.7 | 72.8 | 51.1 | 42.8 | 50.0 | 60.8 | 58.2 | 54.9 | 67.8 | 54.2 | 65.2 | 68.4 | 57.4 |
| pplx-embed-v1-0.6B (INT8) | <u>976</u> | 68.6 | 77.9 | <u>75.6</u> | 60.7 | <u>57.5</u> | 60.1 | 60.1 | 76.6 | 59.9 | 61.2 | 55.0 | 70.8 | 70.3 | 69.5 | 74.3 | 78.6 | 78.7 | 82.1 | <u>65.2</u> |
| pplx-embed-v1-0.6B (BIN) | 7,812 | 64.2 | 73.9 | 71.8 | 54.7 | 54.1 | 53.7 | 55.9 | <u>73.2</u> | 54.9 | 56.0 | 51.2 | 66.0 | <u>67.5</u> | 64.1 | 70.0 | 75.4 | <u>74.5</u> | <u>80.3</u> | 58.7 |
| embed-gemma-0.3B | 325 | 62.3 | 72.8 | 76.0 | <u>56.6</u> | 59.2 | <u>55.9</u> | <u>58.8</u> | 70.3 | <u>58.0</u> | <u>59.7</u> | 51.7 | <u>68.8</u> | 64.1 | 61.8 | 62.6 | 63.1 | 62.8 | 48.5 | 68.0 |
| qwen3-embed-0.6B | 244 | 61.2 | 70.5 | 66.9 | 54.2 | 51.8 | 55.5 | 54.3 | 70.3 | 55.0 | 53.2 | <u>52.4</u> | 63.1 | 62.0 | 61.0 | 49.0 | <u>77.7</u> | 73.9 | 72.1 | 59.2 |

3.1. Public Benchmarks

MTEB Multilingual. The MTEB Multilingual v2 benchmark consists of 131 tasks, of which 18 measure retrieval performance across 146 languages. Table 1 displays the storage efficiency of the embeddings (first column) alongside the average performance across these 18 tasks (second column). Our 4B model, pplx-embed-v1-4B, outperforms gemini-embedding-001 and closely rivals Qwen3-Embedding-4B in terms of average score while being substantially more storage-efficient. Our 0.6B-parameter model, pplx-embed-v1-0.6B, outperforms its Qwen counterpart. We provide per-task evaluation results and details on the evaluation approach in Appendix C.

MIRACL. To provide a more fine-grained illustration of our models’ performance on specific languages, we present the evaluation results on the MIRACL benchmark, a subset of MTEB Multilingual, in Table 2. The MIRACL benchmark evaluates retrieval performance on 18 different languages across several scripts. On this benchmark, pplx-embed-v1-0.6B performs particularly well, outperforming Qwen3-Embedding-0.6B on all language subsets. Even the binarized variant outperforms Qwen3-Embedding-0.6B in terms of average score. Notably, our 0.6B model exceeds the average score of our 4B model. On average, all pplx-embed-v1 models outperform text-embedding-3-large⁶ while trailing Qwen3-Embedding-4B and gemini-embedding-001.

⁶<https://platform.openai.com/docs/guides/embeddings>

Table 3 | Comparison of performance on ConTEB. Models above the line are non-contextualized; models below are contextualized. Dataset abbreviations: Covid (covid-qa), ESG (esg-reports), FB (football), Geo (geography), Ins (insurance), MLDR (mldr), NQA (narrative-qa), SQ (squad). * indicates numbers taken from [Conti et al. \(2025\)](#).

| Model | Avg | Covid | ESG | FB | Geo | Ins | MLDR | NQA | SQ |
|--|--------------|--------------|--------------|--------------|--------------|--------------|--------------|--------------|--------------|
| pplx-embed-v1-4B (INT8) | 58.83 | 63.81 | 47.23 | 34.26 | 73.57 | 14.96 | 79.76 | 81.66 | 75.38 |
| pplx-embed-v1-4B (BIN) | 57.91 | 62.29 | 46.83 | 31.92 | 72.16 | 15.75 | 79.10 | 80.82 | 74.38 |
| pplx-embed-v1-0.6B (INT8) | 55.32 | 63.44 | 42.01 | 29.29 | 63.60 | 10.13 | 79.84 | 80.71 | 73.50 |
| pplx-embed-v1-0.6B (BIN) | 53.29 | 59.59 | 40.13 | 25.96 | 60.83 | 11.09 | 78.95 | 78.63 | 71.12 |
| qwen3-embed-0.6B | 49.36 | 49.10 | 34.72 | 23.15 | 58.11 | 12.65 | 76.27 | 74.02 | 66.85 |
| qwen3-embed-4B | 54.81 | 54.76 | 39.65 | 31.64 | 71.81 | 14.18 | 76.15 | 77.62 | 72.68 |
| pplx-embed-context-v1-4B (INT8) | 81.96 | 62.16 | 62.40 | <u>78.13</u> | 93.04 | 100 | 89.50 | 86.71 | 83.73 |
| pplx-embed-context-v1-4B (BIN) | <u>80.46</u> | 59.60 | <u>58.14</u> | 76.49 | 92.56 | <u>99.69</u> | 88.90 | <u>85.87</u> | 82.67 |
| pplx-embed-context-v1-0.6B (INT8) | 76.53 | 56.21 | 46.92 | 71.43 | 89.38 | 99.28 | 85.99 | 84.13 | 78.91 |
| pplx-embed-context-v1-0.6B (BIN) | 71.69 | 50.28 | 33.85 | 66.35 | 86.99 | 96.23 | 82.84 | 80.54 | 76.40 |
| voyage-context-3 | 79.45 | 55.43 | 54.00 | 79.56 | <u>92.85</u> | 100 | <u>89.24</u> | 81.79 | <u>82.70</u> |
| modernBERT-Large* | 75.6 | 56.0 | 43.1 | 63.9 | 90.7 | 100 | 88.7 | 81.3 | 80.9 |
| anthropic contextual* | 72.4 | <u>60.7</u> | 34.8 | 53.9 | 89.4 | 100 | 85.4 | 77.7 | 77.1 |

MTEB Code. The MTEB Code benchmark comprises 12 retrieval tasks across 15 different programming languages. We present the average performance in the third column of Table 1. While our 4B model performs slightly worse than Qwen3-Embedding-4B, it outperforms text-embedding-3-large and gemini-embedding-001. Moreover, pplx-embed-v1-0.6B outperforms its Qwen3 counterpart. Per-task scores are provided in Appendix C.

ConTEB. We evaluate our models on the ConTEB ([Conti et al., 2025](#)) benchmark using the authors’ evaluation framework `cde_benchmark`⁷, a standardized toolkit for assessing chunk-level retrieval performance. When a contextual model is provided, the toolkit employs late chunking ([Günther et al., 2024](#)) for encoding chunks. In our evaluations, we perform quantization on the pooled chunk embeddings and compute cosine similarity between query embeddings and all document chunk embeddings, ranking chunks by relevance score. Our evaluations are conducted on eight diverse datasets from the ConTEB suite: SQuAD, MLDR, NarrativeQA, Football, COVID-QA, Geography, ESG Reports, and Insurance. Appendix D provides more details of the evaluation process. In Table 3, we provide a comparison of the nDCG@10 metric for contextual and non-contextual models. Our results show that pplx-embed-context-v1-4B yields the best performance while pplx-embed-context-v1-0.6B ranks third, outperforming contextually trained ModernBERT-Large and Anthropic Contextual, but trailing the voyage-context-3 model.

BERGEN. To demonstrate the effectiveness of pplx-embed-v1 in large-scale RAG pipelines, we present evaluations on the BERGEN benchmark ([Rau et al., 2024](#)). We index the KILT Wikipedia dump ([Petroni et al., 2021](#)), consisting of 24.8 million non-overlapping 100-word passages, using pplx-embed-v1, Qwen3-Embedding, and BGE-M3. Following the recommendation of [Rau et al. \(2024\)](#), we evaluate the five question-answering tasks that benefit most from retrieval augmentation: ASQA, HotpotQA, NQ, TriviaQA, and PopQA. For each question, the top-5 retrieved passages are presented to Qwen2.5-32B-

⁷<https://github.com/illuin-tech/conteb>

Table 4 | Match metric on the BERGEN benchmark with **Qwen/Qwen2.5-32B-Instruct** as a generator. No reranking is performed and answers are generated based on the top-5 retrieved passages. The standard retrieval prompt is prepended to queries for Qwen3-Embedding. See Appendix E for details.

| Model | KILT-NQ | KILT-HotpotQA | KILT-TriviaQA | ASQA | PopQA |
|------------------------------------|-------------|---------------|---------------|-------------|-------------|
| pplx-embed-v1-4B (INT8) | 67.7 | 51.9 | 91.9 | 71.5 | <u>68.7</u> |
| pplx-embed-v1-0.6B (INT8) | <u>67.2</u> | <u>51.6</u> | 91.0 | <u>72.6</u> | 70.0 |
| qwen3-embed-4B | 67.1 | 50.2 | <u>91.5</u> | 72.7 | 66.4 |
| qwen3-embed-0.6B | 63.0 | 47.2 | 88.3 | 66.9 | 63.9 |
| bge-m3 | 66.8 | 49.3 | 89.4 | 69.4 | 68.5 |

Table 5 | Results on ToolRet benchmark. All metrics are @10. N=nDCG, P=Precision, R=Recall, C=Comprehensiveness. pplx-embed-v1 is evaluated with INT8 precision.

| Model | Web | | | | Code | | | | Custom | | | | Avg | |
|--------------------|--------------|-------------|--------------|--------------|--------------|-------------|--------------|--------------|--------------|--------------|--------------|--------------|--------------|--------------|
| | N | P | R | C | N | P | R | C | N | P | R | C | N | C |
| bm25 | 26.33 | 6.10 | 34.22 | 22.79 | 41.90 | 6.20 | 56.49 | 55.39 | 41.16 | 8.39 | 48.60 | 38.90 | 36.46 | 39.03 |
| gtr-t5-large | 24.37 | 5.27 | 31.64 | 21.26 | 36.76 | 5.33 | 47.42 | 45.92 | 42.04 | 8.48 | 50.84 | 40.00 | 34.39 | 35.73 |
| gte-base | 30.75 | 7.00 | 39.44 | 25.88 | 41.68 | 6.20 | 53.96 | 51.64 | 37.95 | 6.96 | 46.57 | 38.10 | 36.79 | 38.54 |
| bge-large | 30.03 | 7.01 | 39.28 | 25.63 | 41.53 | 6.00 | 52.76 | 51.18 | 43.90 | 8.31 | 51.79 | 42.24 | 38.49 | 39.68 |
| e5-mistral-7B | 31.07 | 7.65 | 41.30 | 27.04 | 44.97 | 6.66 | 58.95 | 56.79 | 40.88 | 7.91 | 49.35 | 38.35 | 38.97 | 40.73 |
| nv-embed-v1 | 31.51 | 7.74 | 40.52 | 26.74 | 47.92 | 7.10 | 62.07 | 59.60 | 48.70 | <u>10.07</u> | 57.69 | 43.88 | 42.71 | 43.41 |
| gte-qwen2-1.5B | <u>37.53</u> | 9.31 | <u>48.31</u> | <u>30.95</u> | <u>47.38</u> | <u>7.29</u> | <u>61.12</u> | <u>59.55</u> | 52.98 | 10.63 | 59.47 | <u>45.68</u> | 45.96 | 45.39 |
| gritlm-7B | 36.58 | <u>9.34</u> | 46.01 | 27.65 | 41.26 | 6.17 | 53.81 | 52.07 | 45.55 | 9.74 | 54.01 | 41.40 | 41.13 | 40.37 |
| pplx-embed-v1-0.6B | 35.84 | 8.19 | 45.26 | 30.31 | 45.52 | 6.62 | 59.07 | 57.32 | 47.79 | 9.24 | 55.33 | 45.24 | 43.05 | 44.29 |
| pplx-embed-v1-4B | 42.07 | 9.89 | 52.55 | 36.42 | 41.61 | 6.20 | 54.96 | 53.12 | <u>49.68</u> | 9.53 | <u>57.77</u> | 45.98 | <u>44.45</u> | <u>45.17</u> |

Instruct⁸, which generates an answer. In Table 4, we report the match metric, measuring the proportion of generated answers that contain the corresponding ground-truth label. We observe that pplx-embed-v1 performs strongly across all tasks. The pplx-embed-v1-4B model achieves the best results in three of the five tasks, outperforming Qwen3-Embedding-4B in four tasks. We also note that pplx-embed-v1-0.6B outperforms Qwen3-Embedding-4B in three of the five tasks, highlighting its strong performance despite its small size.

Tool Search. We evaluate our models on the ToolRet benchmark (Shi et al., 2025), a comprehensive tool retrieval dataset consisting of 35 tasks across three categories: Web (19 tasks), Code (7 tasks), and Custom (9 tasks). The benchmark contains diverse queries requiring models to retrieve relevant tools from a corpus of API documentation, with evaluation metrics including nDCG@10, Precision@10, Recall@10, and Comprehensiveness@10. As shown in Table 5, our pplx-embed-v1-4B model achieves an average nDCG@10 of 44.45%, ranking second overall among all evaluated models and demonstrating particularly strong performance on the Web category (42.07% nDCG@10). Despite using INT8 quantization, our models remain competitive with larger full-precision baselines, with pplx-embed-v1-0.6B achieving 43.05% average nDCG@10 while being significantly more efficient. Semantic retrieval significantly reduces context explosion by identifying relevant tools from large API corpora, enabling more efficient context management.

⁸<https://huggingface.co/Qwen/Qwen2.5-32B-Instruct>

Table 6 | Query-to-Query Retrieval Performance on PPLXQ2Q Benchmark. Models are grouped by size (separator line at 1B parameters).

| Model ⁹ | Small (240K) | | | Medium (1.2M) | | | Large (2.4M) | | |
|---------------------------|--------------|--------------|--------------|---------------|--------------|--------------|--------------|--------------|--------------|
| | R@10 | R@20 | R@100 | R@10 | R@20 | R@100 | R@10 | R@20 | R@100 |
| pplx-embed-v1-4B (INT8) | 85.04 | 88.15 | 92.75 | 77.47 | 81.87 | 88.55 | 73.46 | 78.26 | 86.17 |
| pplx-embed-v1-4B (BIN) | <u>84.02</u> | <u>87.28</u> | <u>91.98</u> | <u>76.44</u> | <u>80.77</u> | <u>87.69</u> | <u>72.41</u> | <u>77.23</u> | <u>85.21</u> |
| qwen3-embed-4B | 80.90 | 84.57 | 90.21 | 72.36 | 76.96 | 84.90 | 67.90 | 73.02 | 81.96 |
| pplx-embed-v1-0.6B (INT8) | 82.68 | 85.97 | 91.01 | 75.05 | 79.31 | 86.40 | 71.05 | 75.75 | 83.86 |
| pplx-embed-v1-0.6B (BIN) | <u>80.25</u> | <u>83.69</u> | <u>89.01</u> | <u>72.58</u> | <u>76.83</u> | <u>84.11</u> | <u>68.60</u> | <u>73.24</u> | <u>81.42</u> |
| bge-m3 | 73.70 | 77.39 | 84.08 | 65.63 | 69.85 | 77.76 | 61.78 | 66.15 | 74.69 |
| qwen3-embed-0.6B | 68.71 | 73.15 | 81.54 | 59.31 | 64.12 | 73.64 | 55.07 | 59.86 | 69.82 |

3.2. Internal Benchmarks

Public benchmarks are useful, but they do not fully capture web-scale retrieval challenges such as long-tail queries, noisy documents, and distribution shifts in production. To benchmark performance in realistic deployment scenarios, we built PPLX-Query2Query (PPLXQ2Q) and PPLXQuery2Doc (PPLXQ2D), web-scale benchmarks with up to 115K real-world queries spanning a range of difficulty levels, evaluated against more than 30 million documents pooled from over 1 billion web pages. This setup provides a more reliable estimate of recall and ranking performance under realistic corpus sizes and noise.

PPLXQuery2Query. We construct the PPLXQuery2Query benchmark from real search logs spanning five consecutive days from our production search system. Our key insight is that queries leading to the same destination URL exhibit semantic similarity, providing natural supervision for query-to-query retrieval without manual annotation. The construction process proceeds as follows: (1) apply Personally Identifiable Information (PII) detection to exclude any queries that could reveal user identity; (2) collect query-URL pairs from search logs; (3) group queries by destination URL, creating clusters of semantically related queries; (4) filter clusters to retain only those with ≥ 2 queries and remove exact string duplicates; (5) within each cluster, designate the temporally first query as the evaluation query and the remaining queries as pseudo documents. This yields a query set of 100K instances evaluated against document corpora of increasing size (240K, 1.2M, 2.4M), enabling analysis of scale-dependent retrieval performance. Evaluation uses Recall@K ($K \in \{10, 20, 100\}$), where a retrieved document is considered correct if it shares the same destination URL cluster as the query. We compute Recall@K for each query and report the mean across the query set in Table 6.

On the PPLXQ2Q benchmark, pplx-embed-v1 models achieve leading performance in all size categories. On the Large corpus (2.4M target queries), pplx-embed-v1-4B achieves 73.46% R@10 and 86.17% R@100 with INT8 quantization, surpassing Qwen3-Embedding-4B (67.90% R@10, 81.96% R@100) by 5.56 and 4.21 percentage points, respectively. The binary quantized variant maintains strong performance with minimal degradation (72.41% R@10, 85.21% R@100), demonstrating only a 0.96–1.05 percentage point drop while still

⁹Qwen models evaluated using their default prompt as specified in https://huggingface.co/Qwen/Qwen3-Embedding-0.6B/blob/main/config_sentence_transformers.json

Table 7 | Query-to-Document Retrieval Performance on PPLXQuery2Doc Benchmark (English). Models are grouped by size (separator line at 1B parameters).

| Model | Small (7.5M) | | | Medium (15M) | | | Large (30M) | | | |
|---------------------------|--------------|--------------|--------------|--------------|--------------|--------------|--------------|--------------|--------------|--------------|
| | R@10 | R@20 | R@100 | R@10 | R@20 | R@100 | R@10 | R@20 | R@100 | R@1000 |
| pplx-embed-v1-4B (INT8) | 16.29 | 26.00 | 61.38 | 13.76 | 21.84 | 51.05 | 12.18 | 19.22 | 44.26 | 88.23 |
| pplx-embed-v1-4B (BIN) | <u>15.73</u> | <u>25.05</u> | <u>59.97</u> | <u>13.30</u> | <u>20.92</u> | <u>49.52</u> | <u>11.74</u> | <u>18.40</u> | <u>42.82</u> | <u>87.13</u> |
| qwen3-embed-4B | 11.93 | 19.73 | 52.72 | 9.82 | 16.00 | 42.31 | 8.46 | 13.73 | 35.53 | 83.13 |
| pplx-embed-v1-0.6B (INT8) | 14.82 | 23.38 | 56.89 | 12.54 | 19.60 | 46.59 | 11.14 | 17.17 | 40.17 | 84.43 |
| pplx-embed-v1-0.6B (BIN) | <u>13.34</u> | <u>21.31</u> | <u>53.33</u> | <u>11.13</u> | <u>17.62</u> | <u>42.94</u> | <u>9.72</u> | <u>15.27</u> | <u>36.42</u> | <u>80.71</u> |
| bge-m3 | 11.37 | 18.69 | 49.69 | 9.42 | 15.27 | 39.27 | 8.12 | 13.08 | 32.76 | 78.23 |
| qwen3-embed-0.6B | 10.50 | 17.42 | 48.02 | 8.59 | 14.04 | 37.55 | 7.42 | 11.97 | 31.10 | 77.90 |

outperforming all competitors. Similarly, pplx-embed-v1-0.6B achieves 71.05% R@10 and 83.86% R@100, establishing substantial margins over BGE-M3 (61.78% R@10, 74.69% R@100) and Qwen3-Embedding-0.6B (55.07% R@10, 69.82% R@100).

PPLXQuery2Doc. We construct the PPLXQuery2Doc benchmark as follows: (1) We create a high-quality query set using stratified sampling across four dimensions: query intent (Informational, Navigational, Transactional, Factual lookup, Exploratory), query form (Keyword-based, Natural language question, Telegraphic, Long-form verbose), query length (Short: 1–2 tokens, Medium: 3–11 tokens, Long: 12+ tokens), and language distribution to ensure multilingual coverage. (2) For each query, we retrieve documents using four retrieval systems—BM25 (Robertson et al., 2009), BGE-M3 (Chen et al., 2024), Multilingual-e5-large-instruct (Wang et al., 2024), and Qwen3-Embedding-0.6B (Zhang et al., 2025b)—over a corpus of 1 billion real-world web pages. (3) The union of the results from all four systems forms a candidate pool of documents per query. (4) We assign Boolean relevance labels by thresholding Reciprocal Rank Fusion (RRF) scores that aggregate ranking signals from the four retrieval systems and our production search system (which is independent of pplx-embed), ensuring robust relevance judgments through multi-system consensus.

The resulting benchmark comprises 15,000 queries, with 9,380 in English and 5,620 in other languages. Unlike existing public benchmarks that focus on nDCG at small cutoff values, we focus on Recall@K to better reflect real-world cascade search systems where embedding models serve as the first-stage retrieval component. We evaluate across three benchmark sizes: Small (15K queries, 7.5M corpus), Medium (15K queries, 15M corpus), and Large (15K queries, 30M corpus), reporting Recall@10, Recall@20, and Recall@100 across all benchmarks, with additional Recall@1000 reported for the Large benchmark. The corresponding results for English and Multilingual sets are reported in Tables 7 and 8, respectively.

pplx-embed-v1 demonstrates strong performance across both the English and Multilingual variants. On the Large corpus, pplx-embed-v1-4B achieves 88.23% Recall@1000 on English and 91.66% on Multilingual, surpassing Qwen3-Embedding-4B (83.13% and 88.58%, respectively). The binary quantized variants maintain competitive performance with minimal degradation (87.13% and 90.67%, respectively), demonstrating the effectiveness of our quantization-aware training approach. Similarly, pplx-embed-v1-0.6B achieves 84.43% (English) and 89.05% (Multilingual) with INT8 quantization, outperforming all

Table 8 | Query-to-Document Retrieval Performance on PPLXQuery2Doc Benchmark (Multilingual). Models are grouped by size (separator line at 1B parameters).

| Model | Small (7.5M) | | | Medium (15M) | | | Large (30M) | | | |
|---------------------------|--------------|--------------|--------------|--------------|--------------|--------------|--------------|--------------|--------------|--------------|
| | R@10 | R@20 | R@100 | R@10 | R@20 | R@100 | R@10 | R@20 | R@100 | R@1000 |
| pplx-embed-v1-4B (INT8) | 21.05 | 32.35 | 69.70 | 17.87 | 27.14 | 59.19 | 15.58 | 23.80 | 51.84 | 91.66 |
| pplx-embed-v1-4B (BIN) | <u>20.42</u> | <u>31.65</u> | <u>68.56</u> | <u>17.17</u> | <u>26.45</u> | <u>57.73</u> | <u>14.97</u> | <u>23.05</u> | <u>50.42</u> | <u>90.67</u> |
| qwen3-embed-4B | 17.73 | 27.80 | 64.08 | 14.93 | 23.18 | 53.36 | 13.06 | 20.19 | 46.47 | 88.58 |
| pplx-embed-v1-0.6B (INT8) | 19.51 | 29.92 | 66.30 | 16.29 | 24.97 | 55.58 | 14.33 | 21.90 | 48.40 | 89.05 |
| pplx-embed-v1-0.6B (BIN) | <u>17.66</u> | <u>27.44</u> | <u>62.56</u> | <u>14.78</u> | <u>22.69</u> | <u>51.59</u> | <u>12.96</u> | <u>19.73</u> | <u>44.38</u> | <u>85.61</u> |
| bge-m3 | 16.57 | 26.16 | 60.14 | 13.60 | 21.42 | 49.18 | 11.80 | 18.46 | 42.14 | 83.33 |
| qwen3-embed-0.6B | 16.23 | 25.31 | 59.40 | 13.45 | 20.78 | 48.45 | 11.68 | 17.97 | 41.55 | 84.27 |

sub-1B competitors by substantial margins. These high recall rates at $K = 1000$ validate the models’ effectiveness as first-stage retrievers in multi-stage ranking pipelines, where maximizing recall is critical for downstream reranking performance.

3.3. Effect of Binary Quantization

Across all benchmarks, the performance loss from binary quantization is considerably higher for pplx-embed-v1-0.6B, whose performance drops by roughly 2–4.4 percentage points, compared to pplx-embed-v1-4B, which only loses up to 1.6 percentage points. The same trend is observed when comparing pplx-embed-context-v1-4B and pplx-embed-context-v1-0.6B, with the 0.6B model losing up to 5 percentage points and the 4B model losing about 1 percentage point when using binary quantization. Besides the difference in the number of parameters, our 4B models may be more resilient to binarization due to their output dimension of 2560, compared to 1024 for pplx-embed-v1-0.6B. This allows our 4B models to preserve more information in their compressed representations, making them less susceptible to the information loss inherent in quantization.

4. Diffusion vs. Autoregressive Pretraining

In this section, we present an ablation study to demonstrate the effectiveness of diffusion pretraining and bidirectional attention. Starting from pretrained base models, we perform a small number of contrastive pair training steps and evaluate the performance of the resulting embedding models. We evaluate four configurations derived from two base models and two pooling strategies. We compare the causally masked Qwen3 base model (denoted as Qwen3) against a bidirectional backbone pretrained with a diffusion objective (denoted as Diffusion). For each backbone, we apply either mean pooling or last-token pooling. The Qwen3 base model remains causally masked during contrastive training, while the diffusion base model uses bidirectional attention throughout training. We perform pair training on English data for less than one epoch. The training loss, presented in Figure 2, serves as an initial indicator of model performance. We find that the model configurations using the bidirectional diffusion backbone achieve substantially lower loss values compared to those initialized with the causally masked Qwen3 model.

In Table 9, we further compare the performance of the four variants on English retrieval tasks consisting of the MTEB(En, v2) benchmark and the English subset of MIRACLRetrievalHardNegatives. We observe that the combination of mean pooling and

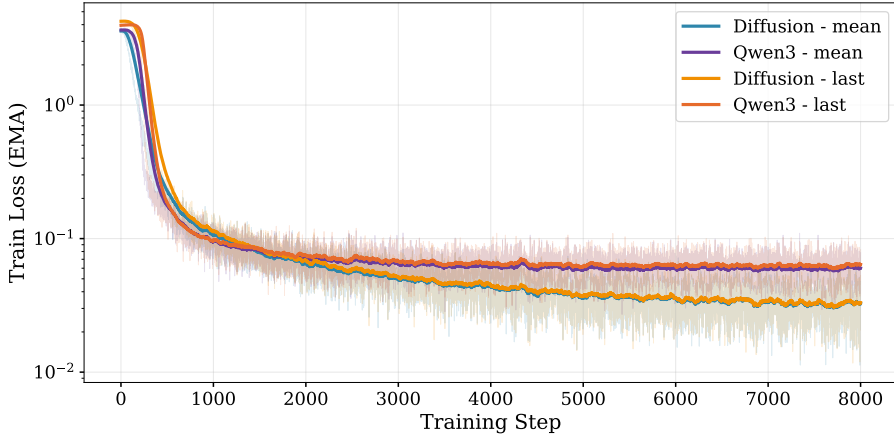
Figure 2 | Smoothed training loss using exponential moving average with $\alpha = 0.02$.

Table 9 | Effect of continued pretraining on selected tasks. Qwen3 refers to the causally masked Qwen/Qwen3-0.6B-Base model, mean and last indicate mean pooling and last-token pooling, respectively. Dataset abbreviations: Game (CQADupstackGamingRetrieval), Unix (CQADupstackUnixRetrieval), DBP (DBpedia), FEV (FEVER), FiQA (FiQA2018), HotQ (HotpotQA), MIR (MIRACLRetrieval), MSM (MSMARCO), NFC (NFCorpus), NQ (NaturalQuestions), SciD (SCIDOCS), SciF (SciFact).

| Base | Pooling | Game | Unix | DBP | FEV | FiQA | HotQ | MIR | MSM | NFC | NQ | SciD | SciF | Avg |
|-----------|---------|-------------|-------------|-------------|-------------|-------------|-------------|-------------|-------------|-------------|-------------|-------------|-------------|-------------|
| Qwen3 | last | 47.7 | 33.2 | 31.2 | 72.1 | 26.6 | 51.7 | 39.3 | 28.3 | 30.9 | 38.6 | 17.1 | 61.5 | 39.9 |
| | mean | 47.2 | 31.4 | 30.3 | 68.1 | 27.0 | 50.5 | 37.8 | 27.3 | 30.2 | 35.5 | 16.8 | 63.0 | 38.8 |
| Diffusion | last | 48.6 | 32.0 | 30.8 | 67.1 | 28.8 | 51.8 | 41.4 | 31.1 | 29.1 | 38.2 | 15.7 | 61.4 | 39.7 |
| | mean | 49.9 | 33.4 | 30.2 | 66.5 | 31.1 | 54.2 | 41.5 | 31.3 | 29.6 | 39.0 | 16.5 | 64.6 | 40.6 |

diffusion pretraining provides improvements on a range of retrieval tasks, resulting in an increase of ~ 1 percentage point on average. In addition to modestly improving benchmark performance, mean pooling is crucial for our contextual embedding training, as it enables computing many chunk-level representations from a single document.

5. Related Work

Diffusion Language Models. Recent work has explored diffusion language models (DLMs) as an alternative to autoregressive models for text generation (Austin et al., 2021; Gong et al., 2025; Nie et al., 2025b). Moreover, Zhang et al. (2025a) conducted a systematic study of diffusion language models for text embeddings, demonstrating that bidirectional attention is crucial for encoding global context in long and complex documents. In this work, we study continued pretraining with diffusion language models and their performance in text retrieval. As noted by Austin et al. (2021), training DLMs with an absorbing state process closely resembles masked language modeling (Devlin et al., 2019) with randomly sampled masking ratios. In this sense, our approach extends a long line of work in which BERT models have been fine-tuned for retrieval (Chen et al., 2024; Günther et al., 2023; Reimers and Gurevych, 2019).

Contrastive Training of Text Embeddings. InfoNCE-based contrastive learning is the predominant approach for training text embedding models, aligning representations of semantically similar texts while distinguishing dissimilar ones (Gao et al., 2021; Izacard et al., 2022; Neelakantan et al., 2022; Reimers and Gurevych, 2019; Santhanam et al., 2022). Contemporary research focuses on improving sample quality through synthesis of pair data (Chen et al., 2025; Thakur et al., 2024; Zhang et al., 2025b), data cleaning (Thakur et al., 2025), and hard negative mining techniques (Chen et al., 2024). Moreover, multi-stage contrastive training has emerged as an effective strategy for training embedding models (Lee et al., 2025a; Li et al., 2023).

Recent work has integrated quantization into contrastive training, from Contrastive Quant in computer vision (Fu et al., 2022) to EmbeddingGemma’s quantization-aware finetuning for weight-quantized variants (Vera et al., 2025). Huerga-Pérez et al. (2025) perform systematic evaluations of post-training quantization for RAG-based use cases. Our work, in contrast, targets quantization-aware training of embeddings for web-scale retrieval.

Contextual Embeddings. Several approaches have emerged for learning contextual embeddings. Morris and Rush (2025) train document embeddings to be contextualized with respect to their neighboring documents in the batch. In contrast, Günther et al. (2024) propose a training-free approach that captures context by processing the chunks in a single forward pass followed by chunk-level pooling. Furthermore, the Context-aware Text Embedding Benchmark (ConTEB) (Conti et al., 2025) was specifically introduced to evaluate models’ ability to leverage global context. Additionally, the authors propose the in-sequence training approach for chunk-level contrast. Our work builds upon these foundations by employing multi-stage contrastive training with a specialized dual-loss objective, while maintaining compatibility with both MTEB and ConTEB evaluation protocols.

6. Conclusion

This report presented the pplx-embed model family, which builds on diffusion-based language models with bidirectional attention to train embedding models that better capture global document context. Our multi-stage training pipeline progressively shapes text representations for semantic alignment, contextualized chunk encoding relative to full documents, and fine-grained relevance distinctions. We provide four model variants—pplx-embed-v1 and pplx-embed-context-v1 at 0.6B and 4B parameter scales—and show through extensive evaluation on public and internal web-scale benchmarks that they achieve strong retrieval performance while offering practical deployment benefits via native quantization-aware training that directly outputs INT8 and binary embeddings.

Acknowledgments

We thank Ismail Gadzhiev and Alexander Pecheny for their contributions to the PPLX benchmarks and Lequn Chen, Svyatoslav Feldsherov, Kevin Hu, Nandor Licker, Sebastian Sepulveda, and Vladimir Zaytsev for their work on supporting pplx-embed in inference. We also thank Tom Aarsen, Alvaro Bartolome, and Joshua Lochner for integrating pplx-embed with sentence-transformers, text-embeddings-inference, and ONNX.

References

J. Austin, D. D. Johnson, J. Ho, D. Tarlow, and R. van den Berg. Structured denoising diffusion models in discrete state-spaces. In *Advances in Neural Information Processing Systems (NeurIPS)*, pages 17981–17993, 2021.

Y. Bengio, N. Léonard, and A. C. Courville. Estimating or propagating gradients through stochastic neurons for conditional computation. *arXiv preprint arXiv:1308.3432*, 2013.

H. Chen, L. Wang, N. Yang, Y. Zhu, Z. Zhao, F. Wei, and Z. Dou. Little giants: Synthesizing high-quality embedding data at scale. In *Proceedings of the 2025 Conference of the Nations of the Americas Chapter of the Association for Computational Linguistics: Human Language Technologies (Volume 1: Long Papers)*, pages 1392–1411, 2025.

J. Chen, S. Xiao, P. Zhang, K. Luo, D. Lian, and Z. Liu. M3-embedding: Multi-linguality, multi-functionality, multi-granularity text embeddings through self-knowledge distillation. In *Findings of the Association for Computational Linguistics: ACL*, pages 2318–2335, 2024.

M. Conti, M. Faysse, G. Viaud, A. Bosselut, C. Hudelot, and P. Colombo. Context is gold to find the gold passage: Evaluating and training contextual document embeddings. *arXiv preprint arXiv:2505.24782*, 2025.

T. Dao. FlashAttention-2: Faster attention with better parallelism and work partitioning. In *International Conference on Learning Representations (ICLR)*, 2024.

J. Devlin, M. Chang, K. Lee, and K. Toutanova. BERT: pre-training of deep bidirectional transformers for language understanding. In *Proceedings of the Conference of the North American Chapter of the Association for Computational Linguistics (NAACL)*, pages 4171–4186, 2019.

K. C. Enevoldsen, I. Chung, I. Kerboua, M. Kardos, A. Mathur, D. Stap, J. Gala, W. Siblini, D. Krzeminski, G. I. Winata, S. Sturua, S. Utpala, M. Ciancone, M. Schaeffer, D. Misra, S. Dhakal, J. Rystrøm, R. Solomatin, Ö. V. Çagatan, A. Kundu, et al. MMTEB: massive multilingual text embedding benchmark. In *International Conference on Learning Representations (ICLR)*, 2025.

Y. Fu, Q. Yu, M. Li, X. Ouyang, V. Chandra, and Y. Lin. Contrastive quant: quantization makes stronger contrastive learning. In *Proceedings of the 59th ACM/IEEE Design Automation Conference*, pages 205–210, 2022.

T. Gao, X. Yao, and D. Chen. SimCSE: Simple contrastive learning of sentence embeddings. In *Proceedings of the Conference on Empirical Methods in Natural Language Processing (EMNLP)*, pages 6894–6910, 2021.

S. Gong, S. Agarwal, Y. Zhang, J. Ye, L. Zheng, M. Li, C. An, P. Zhao, W. Bi, J. Han, H. Peng, and L. Kong. Scaling diffusion language models via adaptation from autoregressive models. In *International Conference on Learning Representations (ICLR)*, 2025.

M. Günther, J. Ong, I. Mohr, A. Abdessalem, T. Abel, M. K. Akram, S. Guzman, G. Mastrapas, S. Sturua, B. Wang, M. Werk, N. Wang, and H. Xiao. Jina Embeddings 2: 8192-token general-purpose text embeddings for long documents. *arXiv preprint arXiv:2310.19923*, 2023.

M. Günther, I. Mohr, B. Wang, and H. Xiao. Late chunking: Contextual chunk embeddings using long-context embedding models. *arXiv preprint arXiv:2409.04701*, 2024.

N. Huerga-Pérez, R. Álvarez, R. Ferrero-Guillén, A. Martínez-Gutiérrez, and J. Díez-González. Optimization of embeddings storage for rag systems using quantization and dimensionality reduction techniques. *arXiv preprint arXiv:2505.00105*, 2025.

G. Izacard, M. Caron, L. Hosseini, S. Riedel, P. Bojanowski, A. Joulin, and E. Grave. Unsupervised dense information retrieval with contrastive learning. *Transactions on Machine Learning Research (TMLR)*, 2022.

A. Q. Jiang, A. Ziarko, B. Piotrowski, W. Li, M. Jamnik, and P. Miłoś. Repurposing language models into embedding models: Finding the compute-optimal recipe. In *Advances in Neural Information Processing Systems (NeurIPS)*, volume 37, pages 61106–61137, 2024.

A. Kusupati, G. Bhatt, A. Rege, M. Wallingford, A. Sinha, V. Ramanujan, W. Howard-Snyder, K. Chen, S. M. Kakade, P. Jain, and A. Farhadi. Matryoshka representation learning. In *Advances in Neural Information Processing Systems (NeurIPS)*, 2022.

C. Lee, R. Roy, M. Xu, J. Raiman, M. Shoeybi, B. Catanzaro, and W. Ping. NV-Embed: Improved techniques for training LLMs as generalist embedding models. In *International Conference on Learning Representations (ICLR)*, 2025a.

J. Lee, F. Chen, S. Dua, D. Cer, M. Shanbhogue, I. Naim, G. H. Abrego, Z. Li, K. Chen, H. S. Vera, et al. Gemini embedding: Generalizable embeddings from Gemini. *arXiv preprint arXiv:2503.07891*, 2025b.

Z. Li, X. Zhang, Y. Zhang, D. Long, P. Xie, and M. Zhang. Towards general text embeddings with multi-stage contrastive learning. *arXiv preprint arXiv:2308.03281*, 2023.

I. Loshchilov and F. Hutter. Decoupled weight decay regularization. In *International Conference on Learning Representations (ICLR)*, 2019.

B. Messmer, V. Sabolcec, and M. Jaggi. Enhancing multilingual LLM pretraining with model-based data selection. *arXiv preprint arXiv:2502.10361*, 2025.

J. X. Morris and A. M. Rush. Contextual document embeddings. In *International Conference on Learning Representations (ICLR)*, 2025.

N. Muennighoff, N. Tazi, L. Magne, and N. Reimers. MTEB: massive text embedding benchmark. In *Proceedings of the Conference of the European Chapter of the Association for Computational Linguistics (EACL)*, 2023.

N. Muennighoff, H. Su, L. Wang, N. Yang, F. Wei, T. Yu, A. Singh, and D. Kiela. Generative representational instruction tuning. In *International Conference on Learning Representations (ICLR)*, 2025.

A. Neelakantan, T. Xu, R. Puri, A. Radford, J. M. Han, J. Tworek, Q. Yuan, N. Tezak, J. W. Kim, C. Hallacy, et al. Text and code embeddings by contrastive pre-training. *arXiv preprint arXiv:2201.10005*, 2022.

S. Nie, F. Zhu, C. Du, T. Pang, Q. Liu, G. Zeng, M. Lin, and C. Li. Scaling up masked diffusion models on text. In *International Conference on Learning Representations (ICLR)*, 2025a.

S. Nie, F. Zhu, Z. You, X. Zhang, J. Ou, J. Hu, J. Zhou, Y. Lin, J. Wen, and C. Li. Large language diffusion models. In *Advances in Neural Information Processing Systems (NeurIPS)*, 2025b.

G. Penedo, H. Kydlícek, L. B. Allal, A. Lozhkov, M. Mitchell, C. A. Raffel, L. von Werra, and T. Wolf. The FineWeb datasets: Decanting the web for the finest text data at scale. In *Advances in Neural Information Processing Systems (NeurIPS)*, 2024.

G. Penedo, H. Kydlícek, V. Sabolcec, B. Messmer, N. Foroutan, A. H. Kargaran, C. Raffel, M. Jaggi, L. von Werra, and T. Wolf. FineWeb2: one pipeline to scale them all - adapting pre-training data processing to every language. *arXiv preprint arXiv:2506.20920*, 2025.

F. Petroni, A. Piktus, A. Fan, P. Lewis, M. Yazdani, N. De Cao, J. Thorne, Y. Jernite, V. Karpukhin, J. Maillard, V. Plachouras, T. Rocktäschel, and S. Riedel. KILT: a benchmark for knowledge intensive language tasks. In *Proceedings of the Conference of the North American Chapter of the Association for Computational Linguistics (NAACL)*, 2021.

D. Rau, H. Déjean, N. Chirkova, T. Formal, S. Wang, S. Clinchant, and V. Nikoulina. BERGEN: A benchmarking library for retrieval-augmented generation. In *Findings of the Association for Computational Linguistics: EMNLP*, 2024.

N. Reimers and I. Gurevych. Sentence-BERT: Sentence embeddings using Siamese BERT-Networks. In *Proceedings of the 2019 Conference on Empirical Methods in Natural Language Processing and the 9th International Joint Conference on Natural Language Processing, EMNLP-IJCNLP 2019*, pages 3980–3990, 2019.

S. Robertson, H. Zaragoza, et al. The probabilistic relevance framework: BM25 and beyond. *Foundations and trends® in information retrieval*, 3(4):333–389, 2009.

K. Santhanam, O. Khattab, J. Saad-Falcon, C. Potts, and M. Zaharia. ColBERTv2: Effective and efficient retrieval via lightweight late interaction. In *Proceedings of the Conference of the North American Chapter of the Association for Computational Linguistics (NAACL)*, pages 3715–3734, 2022.

J. Shi, K. Han, Z. Wang, A. Doucet, and M. K. Titsias. Simplified and generalized masked diffusion for discrete data. In *Advances in Neural Information Processing Systems (NeurIPS)*, 2024.

Z. Shi, Y. Wang, L. Yan, P. Ren, S. Wang, D. Yin, and Z. Ren. Retrieval models aren't tool-savvy: Benchmarking tool retrieval for large language models. In *Proceedings of the Annual Meeting of the Association for Computational Linguistics (ACL)*, 2025.

K. Shoemake. Animating rotation with quaternion curves. In *Proceedings of the 12th Annual Conference on Computer Graphics and Interactive Techniques*, 1985.

Y. Tang and Y. Yang. Pooling and attention: What are effective designs for LLM-based embedding models? *arXiv preprint arXiv:2409.02727*, 2024.

N. Thakur, J. Ni, G. Hernandez Abrego, J. Wieting, J. Lin, and D. Cer. Leveraging LLMs for synthesizing training data across many languages in multilingual dense retrieval. In *Proceedings of the Conference of the North American Chapter of the Association for Computational Linguistics (NAACL)*, pages 7699–7724, 2024.

N. Thakur, C. Zhang, X. Ma, and J. Lin. Hard negatives, hard lessons: Revisiting training data quality for robust information retrieval with LLMs. In *Findings of the Association for Computational Linguistics: EMNLP*, pages 9064–9083, 2025.

H. S. Vera, S. Dua, B. Zhang, D. Salz, R. Mullins, S. R. Panyam, S. Smoot, I. Naim, J. Zou, F. Chen, et al. EmbeddingGemma: Powerful and lightweight text representations. *arXiv preprint arXiv:2509.20354*, 2025.

L. Wang, N. Yang, X. Huang, L. Yang, R. Majumder, and F. Wei. Multilingual E5 text embeddings: A technical report. *arXiv preprint arXiv:2402.05672*, 2024.

A. Yang, A. Li, B. Yang, B. Zhang, B. Hui, B. Zheng, B. Yu, C. Gao, C. Huang, C. Lv, C. Zheng, D. Liu, F. Zhou, F. Huang, F. Hu, H. Ge, H. Wei, H. Lin, J. Tang, J. Yang, J. Tu, J. Zhang, J. Yang, J. Yang, J. Zhou, J. Lin, K. Dang, K. Bao, K. Yang, L. Yu, L. Deng, M. Li, M. Xue, M. Li, P. Zhang, P. Wang, Q. Zhu, R. Men, R. Gao, S. Liu, S. Luo, T. Li, T. Tang, W. Yin, X. Ren, X. Wang, X. Zhang, X. Ren, Y. Fan, Y. Su, Y. Zhang, Y. Zhang, Y. Wan, Y. Liu, Z. Wang, Z. Cui, Z. Zhang, Z. Zhou, and Z. Qiu. Qwen3 technical report. *arXiv preprint arXiv:2505.09388*, 2025.

J. Ye, Z. Xie, L. Zheng, J. Gao, Z. Wu, X. Jiang, Z. Li, and L. Kong. Dream 7B: Diffusion large language models. *arXiv preprint arXiv:2508.15487*, 2025.

S. Zhang, Y. Zhao, L. Geng, A. Cohan, L. A. Tuan, and C. Zhao. Diffusion vs. autoregressive language models: A text embedding perspective. In *Proceedings of the Conference on Empirical Methods in Natural Language Processing (EMNLP)*, pages 4273–4303, 2025a.

X. Zhang, N. Thakur, O. Ogundepo, E. Kamalloo, D. Alfonso-Hermelo, X. Li, Q. Liu, M. Rezagholizadeh, and J. Lin. MIRACL: A multilingual retrieval dataset covering 18 diverse languages. *Transactions of the Association for Computational Linguistics*, 11: 1114–1131, 2023.

Y. Zhang, M. Li, D. Long, X. Zhang, H. Lin, B. Yang, P. Xie, A. Yang, D. Liu, J. Lin, et al. Qwen3 Embedding: Advancing text embedding and reranking through foundation models. *arXiv preprint arXiv:2506.05176*, 2025b.

Appendix

A. Details on Continued Pretraining

Loss. We perform diffusion pretraining via the standard evidence lower bound (ELBO) for a noise process in which tokens decay to an absorbing [MASK] state under a linear noise schedule. Given a sequence x_0 of length L , this forward process is modeled at timestep $t \in [0, 1]$ by $q(x_t|x_0)$, where each token of the noisy sequence x_t has decayed to the absorbing state independently with probability t . We model the reverse process with our bidirectional transformer p_θ . Indexing the l^{th} position of the sequence x_t via the notation x_t^l , we formulate the loss as:

$$\mathcal{L}^{\text{ELBO}}(x_0) = \mathbb{E}_{t \sim \mathcal{U}(0.001, 1)} \left[\frac{1}{t} \mathbb{E}_{q(x_t|x_0)} \left[- \sum_{l=2}^L \delta_{x_t^l, [\text{MASK}]} \log p_\theta(x_0^l|x_t) \right] \right].$$

Here, $\delta_{x_t^l, [\text{MASK}]}$ denotes the Kronecker delta, taking the value 1 at masked positions and the value 0 otherwise. We note that the transformer p_θ maintains a left-shift operation, and we do not prepend a [BOS] token to input sequences. Hence, we cannot make predictions for the first token of the masked sequence and the sum consequently runs only over the last $L - 1$ positions.

Hyperparameters. We perform pretraining using automatic mixed bfloat16 precision and the FlashAttention-2 (Dao, 2024) implementation. The AdamW optimizer uses a weight decay of 0.01, and we set the exponential decay rates to $\beta_1 = 0.9$ and $\beta_2 = 0.98$. We apply gradient clipping based on the ℓ^2 norm of the gradients. Since the appropriate clipping threshold depends on implementation details (e.g., loss scaling), we do not state it here. The learning rate is warmed up linearly over the first 6,000 steps and decayed in a cosine schedule over the last 12,000 steps.

Data. In Table 10, we list the composition of the pretraining data. We fix the prevalence of non-English languages according to their relative word count in the FineWeb2 corpus (Penedo et al., 2025).

B. Details on Contrastive Training

The data used for each of our training stages differ in format, size, and language distribution. To improve the quality of in-batch negatives, a single batch is made up of data from a single dataset; the target dataset is selected randomly with probability proportional to the size of the dataset.

Pair Training. Our models are trained using contrastive learning with InfoNCE loss, where each query uses all in-batch negative documents and all other queries as negatives, with a temperature of 0.02. Critically, we apply INT8 tanh quantization from the beginning

Table 10 | Composition of pretraining data.

| Language | Script | Source | Prevalence |
|----------|--------|-------------|------------|
| eng | Latn | FineWeb-Edu | 50.00% |
| rus | Cyrl | FineWeb2-HQ | 9.22% |
| cmn | Hani | FineWeb2-HQ | 8.51% |
| jpn | Jpan | FineWeb2-HQ | 5.19% |
| deu | Latn | FineWeb2-HQ | 4.11% |
| spa | Latn | FineWeb2-HQ | 4.10% |
| fra | Latn | FineWeb2-HQ | 3.46% |
| ita | Latn | FineWeb2-HQ | 2.18% |
| por | Latn | FineWeb2-HQ | 1.72% |
| nld | Latn | FineWeb2-HQ | 1.17% |
| pol | Latn | FineWeb2-HQ | 1.15% |
| ind | Latn | FineWeb2-HQ | 0.94% |
| vie | Latn | FineWeb2-HQ | 0.80% |
| kor | Hang | FineWeb2 | 0.76% |
| tur | Latn | FineWeb2-HQ | 0.66% |
| fas | Arab | FineWeb2-HQ | 0.62% |
| ces | Latn | FineWeb2-HQ | 0.56% |
| swe | Latn | FineWeb2-HQ | 0.56% |
| ron | Latn | FineWeb2 | 0.55% |
| arb | Arab | FineWeb2-HQ | 0.51% |
| nob | Latn | FineWeb2 | 0.50% |
| hun | Latn | FineWeb2-HQ | 0.48% |
| dan | Latn | FineWeb2-HQ | 0.44% |
| ukr | Cyrl | FineWeb2 | 0.40% |
| tha | Thai | FineWeb2 | 0.39% |
| ell | Grek | FineWeb2-HQ | 0.36% |
| fin | Latn | FineWeb2 | 0.32% |
| hin | Deva | FineWeb2 | 0.18% |
| ben | Beng | FineWeb2 | 0.10% |
| zsm | Latn | FineWeb2 | 0.09% |

of training, enabling the models to learn representations optimized for reduced precision. Both `pplx-embed-v1-0.6B` and `pplx-embed-v1-4B` are trained with a global batch size of 16,384 for 50,000 steps at a sequence length of 256 tokens. We use learning rates of 2×10^{-4} and 5×10^{-5} for the 0.6B and 4B models, respectively, selected to balance training stability and convergence speed across different model scales.

Contextual Training. We train both models initialized from the checkpoint obtained after pair training with quantization applied during both training and inference. The training corpus comprises four contextual retrieval datasets: synthetic MLDR (LLM-generated queries), MLDR, NarrativeQA, and SQuAD, all formatted with chunk-level annotations for contextual embedding learning. Additionally, we synthesize queries for MLDR chunks lacking associated queries. During synthesis, we incorporate neighborhood information into our prompts to prevent generating queries relevant to multiple chunks. Documents are partitioned into chunks of 256 tokens with a fixed number of 16 chunks per document.

We employ a hybrid Matryoshka (Kusupati et al., 2022) dual-objective loss that combines global document-level InfoNCE with a local loss, training in six embedding dimensions [128, 256, 512, 1024, 2048, 2560] with equal weighting. The dual objective weight β is scheduled from 0.2 to 0.5 during training using a cosine annealing schedule. To mitigate false negatives, we implement three masking strategies: relative similarity thresholding to mask negatives within 0.1 of the positive similarity, duplicate document masking, and query-query false negative masking where additional query-query similarities serve as hard negatives for the global loss. Training runs for 7,000 steps with AdamW optimization (learning rate 10^{-5} , weight decay 0.1) and gradient clipping at 1.0. The 0.6B and 4B models are trained with batch sizes of 128 and 16, respectively. The temperature is set to 0.02.

Triplet Training. We perform triplet training using an InfoNCE loss. In this stage, each query uses in-batch negative documents augmented with 3 mined hard negatives. We increase the sequence length to 512 tokens and use a global batch size of 512 with gradient accumulation of 4. The temperature is set to 0.03. Both models are fine-tuned for 2,000 steps, with learning rates of 5×10^{-5} and 10^{-5} for the 0.6B and 4B models, respectively.

C. Details on MTEB Evaluation

We provide per-task scores for the MTEB(Multilingual, v2) retrieval benchmark in Table 11 and per-task scores for the MTEB(Code) benchmark in Table 12. We evaluate `pplx-embed-v1` with a sequence length of 1024 on all tasks except LEMBPasskeyRetrieval, where we use a sequence length of 16,384. We observe that the SyntheticText2SQL task contains duplicate documents in its corpus. To break the symmetry between these duplicates, we inject small random noise into our embeddings. Since the ArguAna task requires the embedding model to find *refuting* documents instead of supporting ones, we find that prepending queries for this task with the string "`Given a claim, find documents that refute the claim. Claim:` " substantially improves performance. Due to the special structure of ArguAna, it is the only dataset where we apply a prompt.

Table 11 | nDCG@10 on MTEB(Multilingual, v2) retrieval tasks

| Task | qwen3-embed-4B | text-embedding-3-large | gemini-embedding-001 | pplx-embed-v1-4B (INT8) | pplx-embed-v1-4B (BIN) | qwen3-embed-0.6B | pplx-embed-v1-0.6B (INT8) | pplx-embed-v1-0.6B (BIN) |
|---------------------------------|----------------|------------------------|----------------------|-------------------------|------------------------|------------------|---------------------------|--------------------------|
| Average | 69.60 | 59.27 | 67.71 | 69.66 | 68.22 | 64.65 | 65.41 | 61.44 |
| AILAStatutes | 81.19 | 41.85 | 48.77 | 61.00 | 60.26 | 79.02 | 59.84 | 53.77 |
| ArguAna | 75.64 | 57.99 | 86.44 | 69.99 | 67.81 | 70.96 | 65.94 | 61.07 |
| BelebeleRetrieval | 81.16 | 68.79 | 90.73 | 77.88 | 76.74 | 68.74 | 72.86 | 68.99 |
| CovidRetrieval | 87.37 | 68.43 | 79.13 | 77.50 | 76.98 | 84.76 | 77.37 | 74.35 |
| HagridRetrieval | 98.77 | 99.04 | 99.31 | 98.77 | 98.77 | 98.76 | 98.77 | 98.77 |
| LEMBPasskeyRetrieval | 84.25 | 69.75 | 38.50 | 89.50 | 79.25 | 84.75 | 76.75 | 60.25 |
| LegalBenchCorporateLobbying | 95.42 | 95.22 | 95.98 | 94.85 | 93.78 | 94.52 | 94.36 | 93.01 |
| MIRACLRetrievalHardNegatives | 69.49 | 56.94 | 70.42 | 66.24 | 64.64 | 61.23 | 68.56 | 64.21 |
| MLQARetrieval | 81.92 | 73.25 | 84.16 | 83.34 | 81.77 | 72.79 | 78.98 | 74.83 |
| SCIDOCS | 31.44 | 23.07 | 25.15 | 23.87 | 23.33 | 24.41 | 22.83 | 21.70 |
| SpartQA | 20.15 | 7.44 | 10.30 | 23.30 | 22.04 | 10.58 | 9.17 | 7.60 |
| StackOverflowQA | 94.32 | 92.44 | 96.71 | 93.61 | 93.08 | 89.99 | 90.65 | 88.97 |
| StatcanDialogueDatasetRetrieval | 42.28 | 31.10 | 51.11 | 56.53 | 55.56 | 33.63 | 41.14 | 34.79 |
| TRECCOVID | 92.92 | 79.56 | 86.32 | 85.61 | 83.94 | 90.52 | 85.90 | 81.33 |
| TempReasonL1 | 1.23 | 2.13 | 2.96 | 1.19 | 1.16 | 1.02 | 1.43 | 1.40 |
| TwitterHjerneRetrieval | 72.58 | 81.44 | 98.02 | 75.67 | 75.24 | 60.04 | 70.04 | 65.20 |
| WikipediaRetrievalMultilingual | 91.23 | 89.24 | 94.20 | 92.68 | 92.30 | 87.13 | 90.98 | 89.74 |
| WinoGrande | 51.51 | 29.11 | 60.52 | 82.40 | 81.28 | 50.79 | 71.85 | 65.92 |

Table 12 | nDCG@10 on MTEB(Code) retrieval tasks

| Task | qwen3-embed-4B | text-embedding-3-large | gemin-embedding-001 | pplx-embed-v1-4B (INT8) | pplx-embed-v1-4B (BIN) | qwen3-embed-0.6B | pplx-embed-v1-0.6B (INT8) | pplx-embed-v1-0.6B (BIN) |
|----------------------------|----------------|------------------------|---------------------|-------------------------|------------------------|------------------|---------------------------|--------------------------|
| Average | 80.07 | 66.54 | 76.00 | <u>78.73</u> | 78.11 | <u>75.42</u> | 75.85 | 73.91 |
| AppsRetrieval | <u>89.18</u> | 28.46 | 93.75 | 87.81 | 86.65 | <u>75.34</u> | 78.66 | 71.70 |
| COIRCodeSearchNetRetrieval | 87.93 | 75.54 | 81.06 | <u>84.39</u> | 83.70 | 84.69 | <u>82.38</u> | 80.15 |
| CodeEditSearchRetrieval | 76.49 | 71.11 | 81.61 | <u>81.26</u> | 80.23 | 64.42 | 76.36 | 72.88 |
| CodeFeedbackMT | 93.21 | 68.92 | 56.28 | <u>86.17</u> | 85.67 | 90.82 | <u>82.96</u> | 81.79 |
| CodeFeedbackST | 89.51 | 80.42 | 85.33 | <u>86.95</u> | 86.52 | 86.39 | <u>84.73</u> | 83.26 |
| CodeSearchNetCCRetrieval | 95.59 | 73.18 | 84.69 | <u>92.27</u> | 91.67 | 91.72 | <u>88.10</u> | 86.04 |
| CodeSearchNetRetrieval | 92.34 | 90.50 | <u>91.33</u> | 90.81 | 90.54 | 91.01 | <u>89.86</u> | 88.73 |
| CodeTransOceanContest | 90.99 | 84.25 | <u>89.53</u> | 88.38 | 88.61 | 86.05 | <u>85.03</u> | 84.86 |
| CodeTransOceanDL | 35.04 | <u>34.23</u> | 31.47 | 33.91 | 33.11 | 31.36 | <u>35.16</u> | 35.36 |
| CosQA | 37.98 | 31.00 | 50.24 | <u>42.34</u> | 41.01 | 36.48 | 43.32 | <u>41.04</u> |
| StackOverflowQA | <u>94.32</u> | 92.44 | 96.71 | 93.61 | 93.08 | <u>89.99</u> | 90.65 | 88.97 |
| SyntheticText2SQL | 78.21 | 68.45 | 69.96 | <u>76.80</u> | 76.52 | 76.74 | 72.98 | 72.18 |

D. Details on ConTEB Evaluation

Our ConTEB evaluation process employs two distinct contextual embedding strategies depending on document characteristics. For standard-length documents, we use the `ContextualEmbedder`, which generates contextual embeddings by incorporating surrounding chunk information during encoding. For exceptionally long documents (notably the ESG Reports dataset, which contains documents exceeding 30,000 tokens), we implement the `FixedContextualEmbedder` with a fixed partitioning strategy that divides documents into overlapping segments of configurable size (default: 10,000 tokens with 35-chunk overlap).

E. Details on BERGEN Evaluation

Embedding Models. Within the BERGEN framework, we implement a custom retriever class that uses the official sentence-transformers implementations of pplx-embed-v1, Qwen3-Embedding, and BGE-M3, ensuring fair evaluations. When encoding queries, we set `prompt_name="query"` for the Qwen3-Embedding models.

RAG Configuration. Below, we provide the command we use for performing the end-to-end RAG evaluations. While the top-100 passages are retrieved from the KILT dump, only the top-5 passages are presented to the generator.

```
python3 -u bergen.py retriever="${retriever}" \
    generator="vllm_qwen-25-32b-instruct" \
    dataset="${dataset}" retrieve_top_k=100 \
    generator.init_args.max_length=32768
```